Eur. J. Mineral.
2002, **14**, 567-574

High-pressure structural behaviour of scolecite

PAOLA COMODI, GIACOMO DIEGO GATTA and PIER FRANCESCO ZANAZZI
Dipartimento di Scienze della Terra, Università di Perugia, Piazza Università, I-06100 Perugia, Italy

Abstract: The H*P* structural evolution of a natural scolecite from Iceland (space group *Cc*) was studied up to 5 GPa using *in situ* single-crystal X-ray diffraction data from a diamond-anvil cell (DAC) with silicon oil as non penetrating pressure transmitting medium. Linear regressions yielded mean axial compressibilities for *a*, *b* and *c* axes of β_a = 4.4(2)·10^{-3}, β_b = 6.1(2)·10^{-3}, β_c = 6.0(1)·10^{-3} GPa^{-1}. K_0, refined with a second-order Birch-Murnaghan equation, fixing K_0' at 4, is 54.6(7) GPa.

The bulk scolecite structure compression was the result of the "soft" behaviour of the channels (K ≅ 17 GPa for [100]-channels; K ≅ 50 GPa for [001]-channels) and the more rigid behaviour of the tetrahedral framework (K ≅ 96 GPa), which underwent kinking of the Secondary Building Unit (SBU) along [100]-chains. The angle between the SBUs (φ), increased from 20.80(2)° at 0.0001 GPa, to 22.00(6)° at 3.38 GPa.

Within the investigated pressure range, the position of the extra-framework cations and water molecules remained almost unchanged. Up to 4.2 GPa no phase transition was observed.

Key-words: zeolite, scolecite, single-crystal X-ray diffraction, high pressure, compressibility.

Introduction

Zeolite minerals are hydrated-framework-alumosilicates which are receiving increasing attention because of their applications in many industrial fields (*e.g.*, pollution control, petroleum production, agricultural application, radioactive waste isolation; Mumpton, 1988; Smyth, 1982; Vaniman & Bish, 1993).

According to Gottardi & Galli (1985) scolecite belongs to the group of "fibrous zeolites". Its ideal chemical composition is $Ca_8Al_{16}Si_{24}O_{80}\cdot 24H_2O$ (Alberti *et al*., 1982).The structure of scolecite under room conditions was determined by Fälth & Hansen (1979) and has been refined by several authors, employing X-ray diffraction or neutron diffraction techniques (Stuckenschmidt *et al*., 1997; Kvick *et al*., 1985; Joswig *et al*., 1984; Smith *et al*., 1984). Its structure is related to those of natrolite (Artioli *et al*., 1984) and mesolite (Adiwidjaja, 1972). The framework is built from tetrahedral chains with topological symmetry $I\bar{4}2d$ running along [100] in the *Cc* space group assumed in the present work, and is characterized by an ordered Si-Al distribution (Fig. 1). The framework shows a rotation of the chains through an angle which is zero only in the ideal symmetrical arrangement, with topological symmetry $I4_1/amd$, but is about 23-24° in natural natrolite and about 35° in dehydrated natrolite (Alberti & Vezzalini, 1981, 1983). The framework encloses two systems of channels: 8-ring channels along [100] and 8-ring channels along [001] (Fig. 1). These channels contain the extra-framework cations and water molecules.

The difference between scolecite, natrolite and mesolite is related to the extra-framework cation and water sites. Natrolite has four sites in the same channels, two of them occupied by Na and the other two occupied by water molecules. The resultant space group is *Fdd*2. For the scolecite, there is only one extra-framework cation site (Ca), preferentially occupied by Ca, and three water molecule sites (W1, W2 and W3). The Ca site in scolecite is coordinated by three water molecules and four framework oxygen atoms in distorted pentagonal bipyramid.

With this configuration, the resultant space group of scolecite is *Cc* or the non-standard *F*1*d*1, for sake of comparison with orthorhombic natrolite and mesolite. The geometrical lattice and structure relations involved in the different choices of unit cells are described by Kvick *et al*. (1985) and Smith *et al*. (1984).

The lower symmetry of scolecite (*Cc* or *F*1*d*1) compared to that of natrolite (*Fdd*2) is the consequence of the distorsion related to a slight rotation of the Si tetrahedra of the chains around the chain axis and 1 Ca site *vs* 2 Na sites. Thus, the channels along [100] become elliptic in order to accommodate the third water molecule (W2).

Because of their industrial importance, and their cation exchange potential, the structural and thermal stability of zeolites have been investigated extensively. There are many single-crystal studies on thermal behaviour of this mineral

*Email: zanazzi@unipg.it

DOI: 10.1127/0935-1221/2002/0014-0567
0935-1221/02/0014-0567 $ 3.60

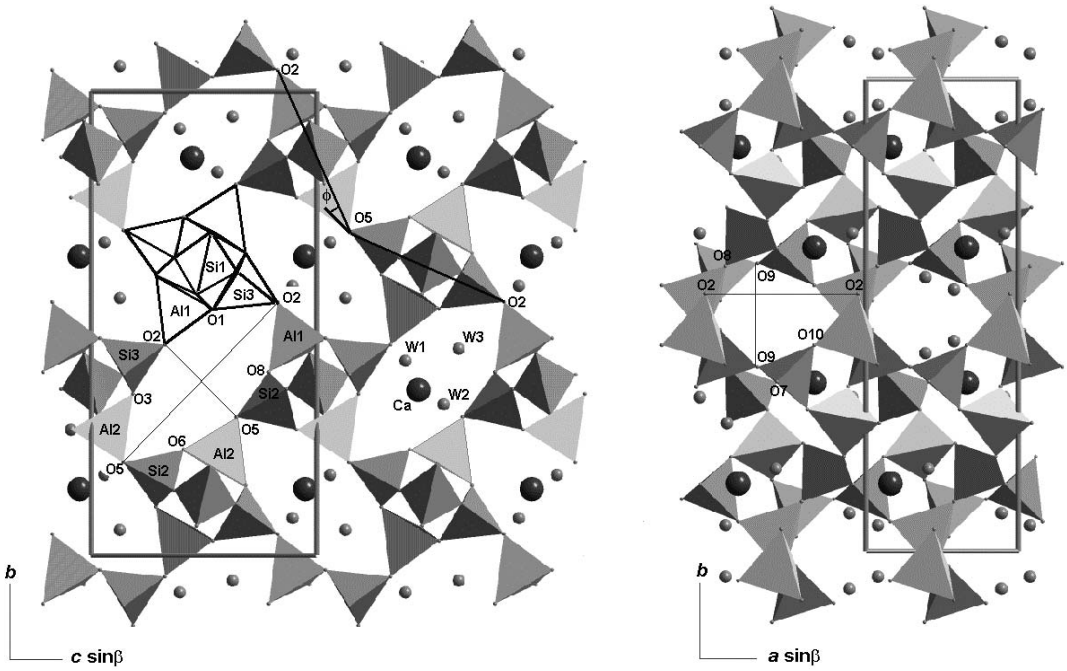

Fig. 1. Projection of scolecite structure viewed down [100] (left), showing the SBU, and viewed down [001] (right). The two channel systems, with the "free diameters" and the extra-framework population are shown. The large spheres represent cation sites, whereas the small spheres represent the oxygen of the water molecules.

group (Alberti & Vezzalini, 1984, and references therein; Vezzalini *et al*., 1993; Alberti *et al*., 1994).

On the other hand, studies of the zeolite structural behaviour under high pressure are scarce, probably due to experimental difficulties and limits. The only single-crystal H*P*-structural data available for natural zeolites is that on heulandite by Comodi *et al*. (2001), who studied the effects of pressure on the framework deformations and the stability of extra-framework sites up to 4 GPa.

It is known that different hydrostatic pressure media have peculiar and important effects on zeolite compressibility. Hazen & Finger (1984) were the first to study the effect of hydrostatic pressure media on the compressibility of a synthetic zeolite 4A using ethanol, methanol, glycerol and organo-fluorine compound. They showed that the compressibility of this zeolite depends on the relative size of the hydrostatic-fluid molecules compared with the structural channels in the zeolite framework. Later Belitsky *et al.* (1992) studied the structural transformations induced by pressure in natrolite and edingtonite using liquids with various molecular dimensions as pressure-transmitting media. Their spectroscopic and diffraction data showed that under high water pressures, some additional H_2O molecules entered the framework channels and caused an anisotropic swelling of the crystal and two phase transitions (natrolite II, natrolite III). Bazhan *et al.* (1997) confirmed the presence of phase transitions induced by high water pressure in scolecite by Raman spectroscopy and optical methods.

Gillet *et al*. (1996) studied pressure-induced amorphization on scolecite and mesolite by synchrotron diffraction in energy-dispersive mode and Raman spectroscopy. In a non-penetrating pressure medium these zeolites showed amorphous-phase transition at 8-9 GPa. The transitions from the crystal to the amorphous phase were irreversible, but in some scolecite experiments during decompression, below 7 GPa, the amorphized samples showed a crystalline rim after removal of pressure.

Recently, Ballone *et al*. (2001) and Vezzalini *et al*. (2001) described the structural modifications of scolecite under high-pressure on the basis of synchrotron powder diffraction and theoretical investigations.

All of the quoted studies on natrolite group (natrolite, edingtonite, scolecite and mesolite) were aimed at studying the H*P*-behaviour using X-ray powder diffraction but did not report structural data. The aim of our study was to investigate the structural evolution of scolecite under pressure by using *in situ* X-ray single-crystal diffraction. The information on the behaviour of scolecite under pressure is compared with the dehydration effect of heating in natrolite-group zeolites.

Experimental method

The scolecite specimen came from Teigarhorn, Iceland. The chemical composition determined with an ARL-SEMQ microprobe (operating conditions: 15 kV, 10 nA measured on brass, beam size 30 μm, 20 s counting time) and the water content measured with thermogravimetric analysis, using DUPONT 951 apparatus (in air, heating rate 10°C/min) at the "Dipartimento di Scienze della Terra" of Modena University, yielded the following chemical formula: $Na_{0.01}Ca_{7.85}(Al_{15.68}Si_{24.32}O_{80})\cdot 24.41H_2O$.

Diffraction data were collected under room conditions on a Philips PW 1100 four-circle diffractometer using a graphite monochromator for Mo*K*α radiation (λ = 0.7107 Å); ω scans with scan width 1.8° and scan speed 0.06°/s were used.

2901 ± *h k l* and ± *h* $\bar{k}$ *l* reflections were measured in the θ range 3-35°. Empirical absorption correction based on the method of North *et al*. (1968) was applied and data were merged to give 1949 independent reflections (R_{eq} = 0.013). 1898 observed reflections with intensities higher than 3σ(I) were employed for the structural refinement (Table 1). The refinement was carried out with anisotropic displacement parameters in space group *Cc* using the SHELX-97 program (Sheldrick, 1997), starting from the atomic coordinates of Smith *et al*. (1984). The final agreement index was 2.01 % for 171 parameters. The neutral atomic scattering factor values from the *International Tables for X-ray Crystallography* (Ibers & Hamilton, 1974) were used. For the channel Ca site the scattering curve of calcium alone was used.

A Merrill-Bassett diamond anvil cell (DAC) with 1/8 carat diamond with 800 μm culet face diameter was used for the high-pressure study. Steel Inconel 750X foil, 250 μm thick, with a 350 μm hole, was used as gasket material. A Sm^{2+}-BaFCl powder for pressure calibration (Comodi & Zanazzi, 1993) and a silicon oil (dimethyl-polysiloxane) as pressure-transmitting medium were introduced into the DAC together with the sample. Silicon oil was chosen because its large-sized molecules do not enter in the zeolite framework channels and for its stability as liquid phase. This medium was used up to *P* greater than 15 GPa at room temperature by Gillet *et al*. (1996) on scolecite powder samples. Anyway, particular care must be devoted in data interpretation because, on the basis of previous experience on the compressibility of silicates, Angel (private communication) pointed out that silicon oil could generate deviatoric stress on the single-crystal sample, as shown by broadening of the diffraction effects over 2.0 GPa.

Pressure was calculated by measuring the wavelength shift of the Sm^{2+} line (λ = 6876 Å, at 0.0001 GPa) excited by a 100 mW argon laser and detected by a 100 cm Jarrell-Ash optical spectrometer. The uncertainties in the pressure measurements were ± 0.05 GPa. A crystal of scolecite with dimensions 120 × 150 × 80 μm was selected for use in the diamond anvil cell.

Table 1. Details of data collection and refinements of scolecite.

Pressure (GPa)	0.0001	1.77	3.38	0.0001*
Radiation	Mo*K*α	Mo*K*α	Mo*K*α	Mo*K*α
θ range (°)	3-35	3-35	3-35	3-35
Scan type	ω	ω	ω	ω
Scan speed (°/s)	0.06	0.06	0.06	0.06
Scan width (°)	1.8	2.6	2.6	2.6
Space group	*Cc*	*Cc*	*Cc*	*Cc*
No. Measured refl.	2901	1427	1601	3045
No. Independent refl.	1949	722	525	1935
No. Observed refl.	1898	306	305	1679
No. Parameters	171	76	76	171
R_{eq}	0.013	0.079	0.105	0.020
R	0.020	0.053	0.062	0.033

* data collected under room conditions after compression.

The lattice parameters were determined at pressures ranging between 0.0001 and 4.21 GPa (Table 2) by applying least-squares method to the Bragg angles of 42 accurately centred reflections measured in several equivalent positions on the diffractometer. The reflections were selected between those with higher intensity in the 2θ range between 14 and 30°.

The intensity data were collected at 1.77 and 3.38 GPa up to θ = 35°, adopting the non-bisecting geometry (Denner *et al*., 1978) and 2.6° ω scans. Intensity data were analysed with a digital procedure (Comodi *et al.*, 1994) and visually inspected to eliminate errors resulting from the overlap of diffraction effects from some parts of the diamond cell or by shadowing from the gasket, and merged into an independent data set. Data were corrected for pressure-cell absorption with an experimental attenuation curve (Finger & King, 1978).

The H*P* structures were refined with isotropic atomic displacement parameters and the site occupancies were fixed as under room conditions. Least-squares refinements were made with the SHELX-97 program (Sheldrick 1997).

Details of the refinements are listed in Table 1. Observed and calculated structure factors can be obtained from the authors upon request (or through the E.J.M. Editorial Office-Paris).

Table 2. Lattice parameters and volumes of scolecite at different pressures.

P (GPa)	*a* (Å)	*b* (Å)	*c* (Å)	*β* (°)	*V* (Å^3)
0.0001	6.533(2)	19.030(3)	9.830(3)	109.95(3)	1148.76(4)
0.37	6.518(3)	18.986(4)	9.790(3)	109.93(3)	1138.96(5)
0.64	6.513(3)	18.961(4)	9.785(3)	109.89(3)	1136.29(5)
0.95	6.499(3)	18.894(4)	9.761(4)	109.88(4)	1127.14(6)
1.52	6.478(4)	18.871(6)	9.730(4)	109.80(4)	1119.14(6)
1.77	6.471(4)	18.804(5)	9.723(5)	109.79(6)	1113.23(6)
2.63	6.451(5)	18.761(6)	9.683(5)	109.67(5)	1103.52(7)
3.38	6.430(4)	18.631(6)	9.636(6)	109.60(6)	1087.48(7)
3.52	6.426(4)	18.620(5)	9.623(4)	109.56(5)	1084.96(8)
3.85	6.418(5)	18.562(6)	9.595(5)	109.55(6)	1077.23(8)
4.04	6.420(5)	18.557(6)	9.583(6)	109.55(6)	1075.86(8)
4.21	6.418(5)	18.544(7)	9.580(6)	109.55(6)	1074.44(9)
0.0001*	6.542(2)	18.842(4)	9.863(4)	109.89(4)	1149.30(5)

* data collected under room conditions after compression.

Table 3. Atomic fractional coordinates, and thermal displacement factors (Å²).

Site	x	y	z	Uiso/Ueq
Ca	0.1613(1)	0.14323(2)	0.0521(1)	0.0132(1)
	0.163(1)	0.1423(4)	0.054(1)	0.012(1)
	0.163(2)	0.1414(5)	0.053(1)	0.010(2)
	0.1610(2)	0.14330(5)	0.0512(2)	0.0122(2)
Si1	0.5	0.37057(3)	0.0	0.0081(1)
	0.5	0.3701(5)	0.0	0.004(2)
	0.5	0.3705(5)	0.0	0.006(2)
	0.5	0.37076(7)	0.0	0.0072(2)
Si2	0.2298(1)	0.33184(3)	0.2001(1)	0.0077(1)
	0.231(2)	0.3333(6)	0.207(2)	0.013(3)
	0.230(2)	0.3342(6)	0.208(2)	0.009(2)
	0.2292(3)	0.33187(7)	0.1996(2)	0.0070(2)
Si3	0.5400(1)	0.08257(3)	0.3312(1)	0.0075(1)
	0.541(2)	0.0835(5)	0.332(2)	0.004(1)
	0.544(2)	0.0839(5)	0.331(2)	0.004(2)
	0.5395(3)	0.08247(6)	0.3307(2)	0.0066(2)
Al1	0.9344(1)	0.46209(3)	0.0998(1)	0.0081(1)
	0.935(2)	0.4628(6)	0.101(2)	0.003(2)
	0.935(2)	0.4628(6)	0.101(2)	0.006(2)
	0.9339(3)	0.46211(8)	0.0991(2)	0.0075(2)
Al2	0.3555(1)	0.21662(3)	0.4338(1)	0.0077(1)
	0.361(2)	0.2185(6)	0.439(2)	0.013(3)
	0.360(2)	0.2189(6)	0.443(2)	0.009(2)
	0.3549(3)	0.21648(7)	0.4334(2)	0.0067(2)
O1	0.5420(3)	0.0315(1)	0.4608(2)	0.0136(3)
	0.548(4)	0.030(1)	0.459(3)	0.018(6)
	0.561(3)	0.031(1)	0.467(3)	0.011(6)
	0.5412(6)	0.0316(2)	0.4607(4)	0.0133(7)
O2	0.4472(3)	0.0460(1)	0.1744(2)	0.0110(3)
	0.445(4)	0.046(1)	0.169(3)	0.020(6)
	0.446(4)	0.048(1)	0.175(4)	0.018(6)
	0.4477(6)	0.0455(2)	0.1738(4)	0.0109(6)
O3	0.3836(3)	0.1513(1)	0.3156(2)	0.0124(3)
	0.387(3)	0.154(1)	0.318(3)	0.007(6)
	0.386(4)	0.153(1)	0.319(3)	0.009(5)
	0.383(6)	0.1516(2)	0.3154(4)	0.0117(6)
O4	0.1154(3)	0.1998(1)	0.4681(2)	0.0130(3)
	0.118(3)	0.201(1)	0.478(3)	0.009(6)
	0.113(4)	0.201(1)	0.473(3)	0.009(5)
	0.1153(6)	0.1995(2)	0.4679(4)	0.0128(7)
O5	0.3535(3)	0.2994(1)	0.3582(2)	0.0105(3)
	0.363(4)	0.303(3)	0.365(3)	0.014(6)
	0.369(4)	0.302(1)	0.371(4)	0.016(6)
	0.3529(6)	0.1993(2)	0.3579(4)	0.0091(6)
O6	0.0868(3)	0.2712(1)	0.0905(2)	0.0126(3)
	0.090(4)	0.271(1)	0.095(3)	0.013(6)
	0.086(4)	0.273(1)	0.098(3)	0.007(5)
	0.0858(6)	0.2713(2)	0.0902(4)	0.0111(6)
O7	0.4143(3)	0.3587(1)	0.1345(2)	0.0139(3)
	0.414(4)	0.360(1)	0.136(3)	0.009(4)
	0.413(4)	0.362(1)	0.137(4)	0.015(5)
	0.4147(6)	0.3586(2)	0.1350(4)	0.0135(7)
O8	0.0767(3)	0.3956(1)	0.2148(2)	0.0135(3)
	0.075(4)	0.397(1)	0.218(3)	0.009(5)
	0.066(4)	0.398(1)	0.222(3)	0.006(5)
	0.0759(6)	0.3957(2)	0.2139(4)	0.0126(6)
O9	0.7894(3)	0.1101(1)	0.3565(2)	0.0128(3)
	0.793(4)	0.113(1)	0.352(3)	0.007(5)
	0.793(4)	0.113(1)	0.352(3)	0.005(5)
	0.7900(6)	0.1095(2)	0.3570(4)	0.0118(6)
O10	0.6602(3)	0.4369(1)	0.0342(2)	0.0141(3)
	0.661(4)	0.437(1)	0.034(3)	0.009(5)
	0.657(4)	0.434(1)	0.033(3)	0.005(5)
	0.6602(6)	0.4369(2)	0.0342(5)	0.0126(6)
W1	0.8908(4)	0.0803(1)	0.1083(3)	0.0316(5)
	0.899(4)	0.077(1)	0.112(4)	0.033(8)
	0.899(5)	0.073(1)	0.109(4)	0.027(7)
	0.8906(8)	0.0807(3)	0.1075(6)	0.031(1)
W2	0.9085(5)	0.3260(1)	0.4404(4)	0.0357(6)
	0.912(4)	0.325(1)	0.438(3)	0.034(7)
	0.910(4)	0.323(1)	0.441(4)	0.030(8)
	0.9077(9)	0.3259(2)	0.4393(7)	0.035(1)
W3	0.5782(4)	0.4454(1)	0.3742(2)	0.0259(5)
	0.587(4)	0.447(2)	0.371(4)	0.032(7)
	0.594(4)	0.447(2)	0.370(4)	0.025(7)
	0.5785(8)	0.4449(2)	0.3743(5)	0.027(1)

Note: For each atom values from top to bottom correspond to the refinement at 0.0001, 1.77, 3.38 and 0.0001 (after decompression) GPa respectively. For H*P* refinements the isotropic thermal parameters, Uiso, are reported, whereas for the room condition refinements Ueq is shown.

Results

Results under room conditions

The coordinates of the framework and extra-framework atoms are given in Table 3. They are very close to those found by Smith *et al*. (1984) for scolecite from Bombay, India. Relevant bond lengths and geometrical parameters related to the size of the channels are listed in Tables 4 and 5. Al and Si are fully ordered into Al1 and Al2, and Si1, Si2 and Si3 sites, with Si-O and Al-O mean distances being 1.620 and 1.746 Å respectively.

Compressibility

The variation of the lattice parameters of scolecite with pressure (Table 2) is shown in Fig. 2, normalized to the value corresponding to room conditions. The reduction of lattice parameters with pressure was linear, without evidence of phase transitions in the pressure range investigated. The compressional pattern is slightly anisotropic. Linear regressions (Fig. 2) yielded mean axial compressibilities for *a*, *b* and *c* axes of $\beta_a = 4.4(2)\cdot10^{-3}$, $\beta_b = 6.1(2)\cdot10^{-3}$, $\beta_c = 6.0(1)\cdot10^{-3}$ GPa^{-1}. As shown in Fig. 2, the β angle decreased slightly with pressure.

Analysis of the strain tensor was performed using the program STRAIN (Ohashi, 1982). Taking the lattice parameters at various pressure, as given in Table 2, resulted in slightly scattered orientations of the strain ellipsoid, owing on the errors of single data. Therefore, an averaged strain tensor was calculated between 1.0 and 4.0 GPa, using the lattice parameter values calculated from linear regression of *P-V* data. The principal axes of the strain ellipsoid were: $\beta_1 = 6.2(2)\cdot10^{-3}$, $\beta_2 = 6.1(1)\cdot10^{-3}$, $\beta_3 = 3.6(4)\cdot10^{-3}$ GPa^{-1}. β_2 was coincident with the *b* axis, whereas β_1 and β_3 lie in the plane (010), β_1 forming an angle of 14 ± 5° with the *c* axis. In other word, the β_1 - β_2 plane is slightly rotated of about 14° from the pseudo-

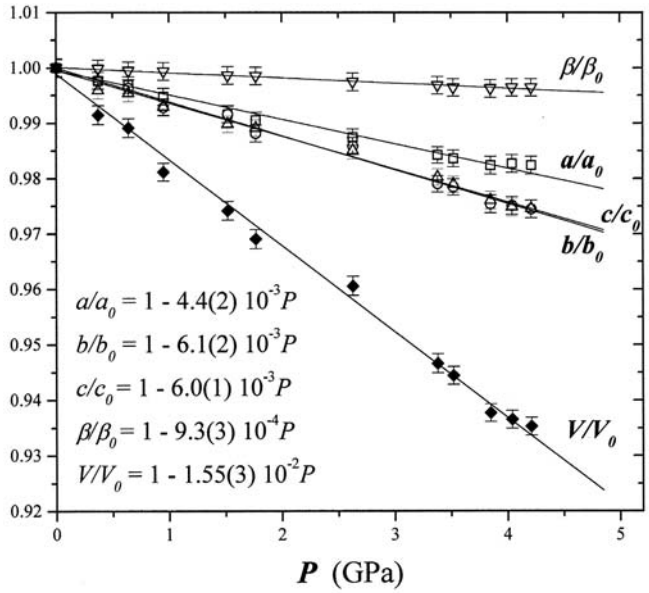

Fig. 2. Unit-cell parameters, normalised to room condition value, *vs*. pressure. The regression line equations are reported in the bottom left-hand corner.

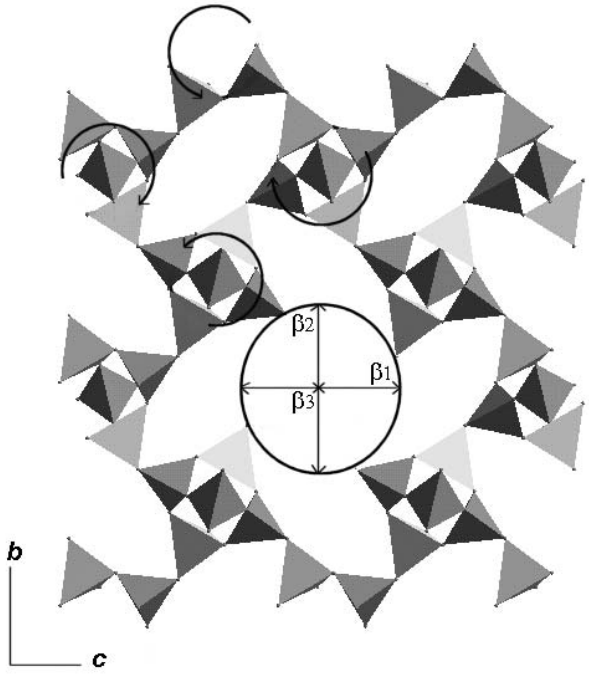

Fig. 3. Strain ellipsoid orientation and cooperative rotation mechanism of SBU under pressure. The β_1 -β_2 plane is rotated along the *b* axis by about 14° from the *bc* plane.

tetragonal plane (100) (Fig. 3). β_1 and β_2 have approximately equal magnitude, as it could be expected taking into account the pseudo-tetragonal symmetry of the framework.

Volume compression data and isothermal bulk modulus K_0 were fitted to a second-order Birch-Murnaghan equation of state, setting K' to its implied value of 4, and using the data weighted by the uncertainties in *P*-*V*. The equation has the form :

$$P = 3/2K_0[(V_0/V)^{7/3} - (V_0/V)^{5/3}]\{1 + 3/4(K_0' - 4)[(V_0/V)^{2/3} - 1]\}$$

and was solved using a Levenberg-Marquardt algorithm (Press *et al*., 1986).

When V_0 and K_0 were refined, the values obtained were: $V_0 = 1148.75(4)$ Å^3, very close to the value measured under room conditions (Table 2), and $K_0 = 54.6(7)$ GPa.

The bulk modulus of scolecite, using a non-penetrating pressure medium, is higher than bulk moduli of other zeolite species, such as zeolite-4A ($K_0 \cong 21$GPa, Hazen & Finger, 1984), and heulandite ($K_0 \cong 27$ GPa, Comodi *et al*., 2001), and is similar to that of sodalite ($K_0 \cong 52$ GPa, Hazen & Sharp, 1988) and marialite ($K_0 \cong 57$ GPa, recalculated from Comodi *et al*., 1990), but is significantly smaller than that observed in other framework silicates (*e.g.*, in meionite (Me68) $K_0 \cong 82$ GPa, recalculated from Comodi *et al.*, 1990; in anorthite, $K_0 \cong 83$ GPa, Hackwell & Angel, 1992; in meionite (Me88), $K_0 \cong 92$ GPa, Hazen & Sharp, 1988).

Structural evolution with pressure

The H*P* structural behaviour of this zeolite type was studied by comparing the three refinements carried out at 0.0001, 1.77 and 3.38 GPa. The pressure increase did not produce relevant variations in the tetrahedral bond distances (Table 4) as observed in most silicates in this

Table 4. Interatomic distances (Å) in function of pressure.

P (GPa)	0.0001	1.77	3.38	0.0001*
Ca-O2	2.608(2)	2.53(2)	2.51(2)	2.618(4)
Ca-O3	2.508(2)	2.49(2)	2.47(3)	2.513(4)
Ca-O5	2.499(2)	2.40(2)	2.35(2)	2.497(4)
Ca-O6	2.571(2)	2.53(2)	2.57(2)	2.534(3)
Ca-W1	2.349(3)	2.32(3)	2.32(3)	2.345(5)
Ca-W2	2.317(3)	2.34(3)	2.30(2)	2.316(5)
Ca-W3	2.355(2)	2.37(3)	2.34(3)	2.343(4)
Si1-O4	1.616(2)	1.59(2)	1.58(2)	1.614(3)
Si1-O7	1.620(2)	1.63(3)	1.59(3)	1.624(4)
Si1-O9	1.641(2)	1.62(3)	1.62(2)	1.637(4)
Si1-O10	1.597(2)	1.59(2)	1.54(2)	1.594(4)
<Si1-O>	1.618	1.60	1.58	1.617
Si2-O5	1.612(2)	1.59(3)	1.62(3)	1.614(3)
Si2-O6	1.634(2)	1.64(2)	1.62(2)	1.633(3)
Si2-O7	1.631(2)	1.62(2)	1.63(3)	1.629(4)
Si2-O8	1.606(2)	1.60(2)	1.63(2)	1.608(3)
<Si2-O>	1.620	1.61	1.62	1.621
Si3-O1	1.600(1)	1.58(2)	1.59(3)	1.600(4)
Si3-O2	1.610(2)	1.65(3)	1.56(3)	1.614(4)
Si3-O3	1.631(2)	1.63(2)	1.63(2)	1.637(3)
Si3-O9	1.645(2)	1.67(2)	1.64(2)	1.647(4)
<Si3-O>	1.621	1.63	1.60	1.624
Al1-O1	1.743(2)	1.77(2)	1.74(3)	1.736(4)
Al1-O2	1.743(2)	1.70(3)	1.73(3)	1.735(3)
Al1-O8	1.738(2)	1.71(2)	1.69(3)	1.734(4)
Al1-O10	1.748(2)	1.73(2)	1.76(2)	1.745(4)
<Al1-O>	1.743	1.73	1.73	1.737
Al2-O3	1.752(2)	1.74(2)	1.74(3)	1.745(3)
Al2-O4	1.742(2)	1.77(2)	1.74(2)	1.741(4)
Al2-O5	1.736(2)	1.74(3)	1.71(3)	1.737(3)
Al2-O6	1.766(2)	1.73(2)	1.70(2)	1.765(4)
<Al2-O>	1.749	1.74	1.72	1.747

* data collected at room conditions after compression.

Table 5. Relevant structural parameters in scolecite at different pressures.

P (GPa)	0.0001	1.77	3.38	0.0001*	K (GPa)
Vol- SBU (Å^3)	22.17(3)	21.91(4)	21.42(4)	22.09(3)	96(6)
Si1-Si1 (Å)	6.527(3)	6.468(5)	6.450(6)	6.527(2)	
Si2-Si3 (Å)	3.781(2)	3.761(6)	3.721(6)	3.781(2)	
Al1-Al2 (Å)	3.723(2)	3.715(5)	3.680(5)	3.720(3)	
φ(°)	20.80(2)	21.85(6)	22.00(6)	20.75(6)	
Channel [001]					
O2-O2 (Å)	3.827(2)	3.768(5)	3.750(4)	3.827(2)	
O7-O10 (Å)	2.666(3)	2.565(4)	2.502(6)	2.663(2)	
O9-O8 (Å)	1.674(3)	1.637(5)	1.612(6)	1.664(3)	
O9-O9 (Å)	3.760(3)	3.750(4)	3.670(5)	3.743(3)	
$V_{ch\ 8\text{-}ring}$ (Å^3)	102.44(4)	100.88(5)	95.88	101.89(3)	50(3)
Channel [100]					
O2-O5 (Å)	6.866(3)	6.872(5)	6.754(6)	6.864(2)	
O3-O6 (Å)	0.603(2)	0.529(4)	0.529(5)	0.602(3)	
O1-O8 (Å)	0.899(4)	0.767(5)	0.728(5)	0.904(3)	
O2-O5 (Å)	2.307(3)	2.131(4)	2.077(5)	2.316(2)	
Al2-O5-Si2 (°)	133.41(1)	130.72(2)	129.42(3)	133.40(2)	
Si3-O2-Al1 (°)	138.21(2)	135.91(3)	136.93(3)	138.61(2)	
O3-O5-O6 (°)	73.23(2)	71.31(4)	71.55(5)	73.39(2)	
O1-O2-O3 (°)	159.90(1)	160.01(3)	160.41(4)	159.81(2)	
O6-O5-O8 (°)	155.40(2)	156.22(3)	155.20(4)	155.42(3)	
O1-O2-O8 (°)	78.92(1)	76.40(2)	76.18(3)	79.23(2)	
$V_{ch\ 8\text{-}ring}$ (Å^3)	49.07(3)	41.52(6)	39.23(7)	49.54(4)	17(2)

* data collected at room conditions after compression.

pressure range. On the other hand, as expected for open framework structures, the main deformation mechanism was the polyhedral tilting that produced inter-tetrahedral angle variations. In particular in scolecite the most relevant structural variations were produced by cooperative rotation of the Secondary Building Units (SBUs) along [100] (Fig. 3). The main effects were observed in the 8-membered ring channels along [100]: the acute angles of the channel ((O3-O5-O6)°, (O1-O2-O8)°) decreased, whereas the obtuse angles ((O1-O2-O3)°, (O6-O5-O8)°) increased (Table 5). The φ angle, defined as φ° = [180°-(O2-O5-O2)°]/2, increased from 20.80(2)° at 0.0001 GPa, to 22.00(6)° at 3.38 GPa (Table 5). At the same time, the 8-membered ring channels, parallel to *a,* were compressed. The [100]-channel bulk modulus, calculated from the volume variations of the inscribed elliptical-section cylinders, was quite low: 17(2) GPa. On the contrary, the effect of the SBUs rotation produced in the 8-membered ring along [001] a minor deformation: the [001]-channel bulk modulus was 50(3) GPa (Table 5).

Besides relevant decrease in the channel free volumes, the pressure increase did not yield important variations in the shape of the channels. We can evaluate the evolution on the channel ellipticity by the ratio between the smaller free diameter compared to the larger one, O5-O2(short)/O5-O2(long) for the 8-ring channel along [100], O9-O9/O2-O2 for the 8-ring channel along [001] (Fig. 1). According to the results shown in Table 5, it appears that the shape of the channels along [001] did not change much with pressure, whereas the channels along [100] increased their ellipticity. In fact, the ratio O9-O9/O2-O2 changed from 0.982 to 0.972 with pressure increase of 3.38 GPa, corresponding to a decrease of about 1 %, while the ratio O5-O2(short)/O5-O2(long) decreased from 0.336 to 0.307, corresponding to a decrease of about 8.6 %.

SBU-rotation not only produced changes in the configuration between building units, but also changed the size of the SBU itself. The SBU volume, calculated considering the SBU as a distorted polyhedron with 6 vertices formed by the centers of the 6 nearest tetrahedra, changed from 22.17(3) Å^3, under room conditions, to 21.42(4) Å^3 at 3.38 GPa. Thus the SBU bulk modulus was 96(6) GPa (Table 5). The bulk scolecite structure compression was therefore the result of the "soft" behaviour of the channels and the more rigid behaviour of the tetrahedral framework.

The position of the extra-framework cations (Ca site) and water molecules (W1, W2, W3 sites) was maintained approximately within the pressure range investigated (Table 3). However, looking in more detail at the evolution of the extra-framework bonding distances, a different behaviour of the distances between Ca cations and framework oxygens and Ca and water molecules appears. In fact, under high-pressure conditions, the distances between Ca and framework oxygens became shorter (the variations with respect to room conditions distances are Ca-O2 -3.7%, Ca-O3 -1.5%, Ca-O5 -5.9%, Ca-O6 ≈ 0%, see Table 4). On the contrary the distances between Ca and water molecules slightly decrease with pressure (Ca-W1 -1.2%), or do not change significantly (Ca-W2 and Ca-W3). In other words, in high pressure conditions, the Ca moves towards the framework, in particular towards the acute angle formed by (O3-O5-O6), where the electronic density is lower, since the water molecules lie on the opposite side of the channel (Fig. 1).

Significant peak broadening was observed at *P* higher than 3.8 GPa. At 4.4 GPa, the peak disappearance hindered

a suitable determination of the lattice parameters. The evolution of the diffraction pattern during decompression showed a partial recovery of the intensity of reflections. Refinement of the structure under room conditions with the sample in air after decompression was still possible, though the intensities measured where about two thirds lower than those of the natural sample. Results showed little difference from the initial values of the lattice parameters and structural geometry (Tables 3-4-5).

The peak broadening could be due to the occurrence of a severe mechanical stress induced by the non hydrostaticity of the silicon oil (Angel, private communication). This hypothesis seems supported by the structure recovery after release of the elastic strain. Another explication could be found assuming that, starting from about 4 GPa, the onset of amorphization was occurring. In effect Ballone *et al.* (2001) and Vezzalini *et al*. (2001) found irreversible amorphization after application of higher pressure, on the basis of synchrotron powder diffraction data. Complete amorphization at 8-9 GPa was observed for scolecite by Gillet *et al*. (1996).

Discussion and conclusions

Following Comodi *et al*.'s (2001) study of heulandite, scolecite represents the second example of natural zeolite studied under pressure using single-crystal X-ray diffraction.

The topological tetragonal symmetry of the framework controls the cooperative rotation of SBUs, explaining the similar compressibility observed for *b* and *c* parameters, in comparison with that of the *a* parameter which shows, as expected, smaller compressibility. The two most compressible directions are oriented along the diagonals of the [100] channel system (Fig. 3), the directions along which the electron density is lower. The deformation mechanism observed in this study confirms the results of ab-initio molecular dynamics simulations by Ballone *et al*. (2001) regarding the structural modifications of scolecite under high-pressure: the mean deformative behaviour is the cooperative rotation of SBUs, leading to a reduction of the channel section.

By comparing the structural deformations induced in scolecite by high pressure, with those induced by high temperature, it is seen that the former are less dramatic. This can be explained by taking into account that an increase in temperature produces dehydration, with partial loss of the water molecules, and rearrangement of the framework and of the extraframework content, leading to phase transitions. The effects of the dehydration processes were shown by the studies of Adiwidjaja (1972) and of Ståhl & Hanson (1994) by real-time synchrotron powder diffraction. Alberti & Vezzalini (1983) studied the H*T* behaviour of natrolite showing how the crystal structure, which was stable under room conditions, was modified through heating-induced dehydration. They proposed a real structure of dehydrated phase at 350-500°C, called "metanatrolite", different from the structure models proposed by Peacor (1973) and Van Reeuwijk (1972, 1974). The significant change in the framework of dehydrated natrolite is related to the rotation of the tetrahedral chains around their long axis; the *a* direction for *Cc* space group. The most evident modification, involving the extraframework cations, is the shift of their positions near to those occupied by water molecules, producing differences in the coordination number of the Na atoms.

On the contrary, in our study the extraframework content remained unchanged with the pressure increase: both cations and water molecules maintained almost the same position and the same occupancy, and no phase transitions were observed in the pressure range investigated.

The analysis of the structural deformations under pressure allows us to hypothesize the mechanism of structural decay towards amorphization observed below 10 GPa by Gillet *et al.* (1996). The cooperative rotation of SBUs causes relevant changes in the T-O-T angles between adjacent tetrahedra. The smallest T-O-T angle, Al2-O5-Si2, is 133.4° under room conditions, and becomes 129.4° at 3.38 GPa (Table 5), differing significantly from the average value of 140° found for a large number of silicates with T-O-T bonds (Liebau, 1961; Brown & Gibbs, 1970) and the theoretical value of 131° estimated by Tossell & Gibbs (1978) on the basis of molecular-orbital calculations on model systems of tetrahedral chains. A further increase of pressure, would bring the two adjacent tetrahedra progressively together, with an increase of potential energy, generating possible instability in the framework structure.

Acknowledgements: Thanks are due to G. Vezzalini and S. Quartieri for the sample of scolecite from Iceland and for the microprobe analysis. The paper greatly benefited from their helpful comments and discussion. The critical and helpful revisions of Dr. M.E. Gunter, H. Yang and of the Ass. Editor R.J. Angel, are gratefully acknowledged. Many thanks are due to H.A. Giles (MA) for editing the English of the paper. This work was financially supported by C.N.R and M.U.R.S.T. (project "Trasformazioni, reazioni, ordinamenti nei minerali") grants to P.F.Z.

References

Adiwidjaja (1972): Strukturbeziehungen in der natrolithgruppe und das entwässerungsverhalten des skolezits. Diss. Univ. Hamburg.

Alberti, A., Pongiluppi, D., Vezzalini, G. (1982): The crystal chemistry of natrolite, mesolite and scolecite. *N. Jb. Miner. Abh*., **143**, 231-248.

Alberti, A., Quartieri, S., Vezzalini, G. (1994): Structural modifications induced by dehydration in yugawaralite. *in* "Zeolite and related microporous materials: state of the art 1994". Studies in surface sciences and catalysis, Vol. 84, Weitkamp, J., Karge, H.G., Pfefer, H. and Holderich, W., eds., Elsevier Science B.V., 637-644.

Alberti, A. & Vezzalini, G. (1981): A partially disordered natrolite: relationships between cell parameters and Si-Al distribution. *Acta Cryst*., **B37**, 781-788.

— , — (1983): How the structure of natrolite is modified through the heating induced dehydration. *N. Jb. Miner. Msh.*, 135-144.

—, — (1984): Topological changes in dehydrated zeolite: breaking of T-O-T oxygen bridges. *in* "Proc. 6th Int. Zeolite Conf. Reno.", Olson, D. & Bisio, A., eds., Buttherworth, Guildford, U.K., 834-841.

Artioli, G., Smith, J.V., Kvick, Å. (1984): A neutron diffraction study of natrolite, $Na_2Al_2Si_3O_{10}$ $2H_2O$ at 20 K. *Acta Cryst*., **C40**, 1658-1662.

Ballone, P., Quartieri, S., Sani, A., Vezzalini, G. (2001): Lattice deformations and structural transitions in zeolite scolecite under pressure: a combined experimental and computational study. *in* "Proc. Istituto Nazionale di Fisica della Materia Meeting", Roma, Italy, *in press*.

Bazhan, I.S., Fursenko, B.A., Kholdeev, O.V. (1997): Scolecite phase transformation at high hydrostatic pressure. *in* "Proc. 5th Int. Zeolite. Conf.", Ischia, Italy, 57-59.

Belitsky, I.A., Fursenko, B.A., Gabuda, S.P., Kholdeev, O.V., Seryotkin, Y.V. (1992): Structural transformation in Natrolite and Edingtonite. *Phys. Chem. Minerals*, **18**, 497-505.

Brown, G.E. & Gibbs, G.V. (1970): Stereochemistry and ordering in the terahedral portion of silicates. *Am. Mineral.,* **55**, 1587-1607.

Comodi, P. & Zanazzi, P.F. (1993): Improved calibration curve for the Sm^{2+}: BaFCl pressure sensor. *J. Appl. Cryst.*, **26**, 843-845.

Comodi, P., Mellini, M., Zanazzi, P.F. (1990): Scapolites: variation of the structure with pressure and possible role in the storage of fluids. *Eur. J. Mineral.*, **2**, 195-202.

Comodi, P., Melacci, P.T., Polidori, G., Zanazzi, P.F. (1994): Trattamento del profilo di diffrazione da campioni in cella ad alta pressione. *in* "Proc. 24th Nat. Cong. of Associazione Italiana di Cristallografia", Pavia, Italy, 119-120.

Comodi, P., Gatta, G. D., Zanazzi, P.F. (2001): High-pressure structural behaviour of heulandite. *Eur. J. Mineral*., **13***,* 497-505.

Denner, W., Schulz, H., d'Amour, H. (1978): A new measuring procedure for data collection with high-pressure cell on X-ray four-circle diffractometer. *J. Appl. Cryst.*, **11**, 260-264.

Fälth, L. & Hansen, S. (1979): Structure of scolecite from Poona, India. *Acta Cryst*., **B35**, 1877-1880.

Finger, L.W. & King, H. (1978): A revised method of operation of the single-crystal diamond cell and refinement of the structure of NaCl at 32 kbar. *Am. Mineral.*, **63**, 337-342.

Gottardi, G. & Galli, E. (1985): Natural Zeolites. Springer-Verlag, Berlin Heidelberg, 409 p.

Gillet, P., Malézieux, J.M., Itié, J.P. (1996): Phase changes and amorphization of zeolites at high pressure: The case of scolecite and mesolite. *Am. Mineral.*, **81**, 651-657.

Hackwell, T.P. & Angel, R.J. (1992): The comparative compressibility of reedmergnerite, danburite and their aluminium analogues. *Eur. J. Mineral.*, **4**, 1221-1227.

Hazen, R.M. & Finger, L.W. (1984): Compressibility of zeolite 4A is dependent on the molecular size of the hydrostatic pressure medium. *J. Appl. Phys.*, **56**(6), 1838-1840.

Hazen, R.M. & Sharp, Z.D. (1988): Compressibility of sodalite and scapolite. *Am. Mineral.*, **73**, 1120-1122.

Kvick, Å., Ståhl, K., Smith, J.V. (1985): A neutron diffraction study of the bonding of zeolitic water in scolecite at 20 K. *Z. Kristallogr*., **171**, 141-154.

Ibers, J.A. & Hamilton, W.C., eds. (1974): International Tables for X-ray Crystallography, vol. IV, Kynoch, Birmingham, U.K.

Joswig, W., Bartl, H., Fuess, H. (1984): Structure refinement of scolecite by neutron diffraction. *Z. Kristallogr*., **166**, 219-223.

Liebau, F. (1961): Untersuchungen über die grösse des Si-O-Si-valenzwinkels. *Acta Cryst*., **14**, 1103-1109.

Mumpton, F.A. (1988): Development of uses for natural zeolites: A critical commentary. *in* "Occurrence, properties and utilization of natural zeolites", Kallo D. & Sherry H.S., eds., Akademiai Kiado, Budapest, Hungary, 333-365.

North, A.C.T., Phillips, D.C., Mathews, F.S. (1968): A semiempirical method of absorption correction. *Acta Cryst.*, **A24**, 351-359.

Ohashi, Y. (1982): A program to calculate the strain tensor from two sets of unit-cell parameters. *in* "Comparative Crystal Chemistry", Hazen, R.M. & Finger, L.W., eds., Wiley, New York, 92-102.

Peacor, D.R. (1973): High-temperature, single-crystal x-ray study of natrolite. *Am. Mineral*., **58**, 676-680.

Press, W.H., Flannery, B.P., Teukolsky, S.A., Vetterling, W.T. (1986): Numerical recipes. Cambridge University Press, Cambridge, U.K., 521-528.

Sheldrick, G.M. (1997): SHELX-97. Programs for crystal structure determination and refinement. Institut für Anorg. Chemie, Univ. of Göttingen, Germany.

Smith, J.V., Pluth, J.J., Artioli, G., Ross, F.K. (1984): Neutron and X-ray refinement of scolecite. *in* "Proc. 6th Int. Zeolite Conf.", Heyden, London, 842-850.

Smyth, J.R. (1982): Zeolite stability and radioactive waste isolation in volcanic rocks. *J. Geol.*, **90**, 195-201.

Ståhl, K. & Hanson, J. (1994): Real-time X-ray synchrotron powder diffraction studies of the dehydration processes in scolecite and mesolite. *J. Appl. Cryst.*, **27**, 543-550.

Stuckenschmidt, E., Joswig, W., Baur, W.H. (1997): Scolecite, part I: refinement of high-order data, separation of internal and external vibrational amplitudes from displacement parameters. *Phys. Chem. Minerals*, **24**, 403-410.

Tossell, J.A. & Gibbs G.V. (1978): The use of molecular-orbital calculations on model systems for the prediction of bridging-bond-angle variations in siloxanes, silicates, silicon nitrides and silicon sulfides. *Acta Cryst*., **A34**, 463-472.

Vaniman, D.T. & Bish, D.L. (1993): The importance of zeolite in the potential high-level radioactive waste repository at Yucca Mountain, Nevada. *in* "Natural Zeolites '93", Ming, D.M. & Mumpton, F.A., eds., Int. Comm. Natural Zeolites, Brockport, New York, 533-546.

Van Reeuwijk, L.P. (1972): High temperature phases of zeolites of the natrolite group. *Am. Mineral*., **57**, 499-510.

— (1974): The thermal dehydration of natural zeolites. Meded Landbouwhogeschool Wageningen, Netherlands.

Vezzalini, G., Quartieri, S., Alberti, A. (1993): Structural modifications induced by dehydration in the zeolite gismondine. *Zeolites*, **13**, 34-42.

Vezzalini G., Quartieri S., Sani A., Levy D. (2001): Structural modifications induced by high pressure in scolecite and heulandite: *in-situ* synchrotron X-ray Powder diffraction study. *in* "Proc. 13th Int. Zeolite Conf.", Montpellier, France, *in press.*

Received 1 June 2001
Modified version received 8 October 2001
Accepted 7 November 2001